H_2), but this spacing does vary with the nature of the partial oxidation of the M(pc) rings (Table VI). For example in Co(pc)I partial oxidation occurs at the metal center rather than the ring, and the compound thus is a metal-spine conductor. Bonding interactions between partially oxidized $Co^{2.33}$ centers in Co(pc)I substantially shorten the Co–Co distance to 3.123 (1) Å.[5]

Although Br atoms are smaller and Br_3^- chains shorter than their iodine analogues, the intrastack spacing in Ni(pc)Br is no shorter than that of Ni(pc)I. Viewed another way, there is room for ca. 13% more Br_3^- than I_3^- in the channels between phthalocyanine stacks. Since Br_2 is a stronger oxidant than I_2, further oxidation of the Ni(pc) system is favored. Yet the halogen to Ni(pc) ratio of 1:1 and the degree of oxidation, $^1/_3$ electron/Ni(pc) ring, are the same for oxidation by Br_2 and I_2. Thus the size and structure of the counterion do not determine the degree of oxidation, but rather it appears that the degree of charge transfer is largely a function of the crystal structure as dictated by the donor units. This finding is in accord with other studies[19] of metallophthalocyanine donors in combination with various dopants of different sizes and structures, such as TCNQ, DDQ, BF_4^-, and PF_6^-,[20] where the maximum dopant level is invariably $\sim ^1/_3$. However, these studies are complicated by problems of inhomogeneous doping. Euler[21] has suggested that the rotation angle between adjacent phthalocyanine rings is determined by the size of the counterion and that the angle will constrict to ~35° for Ni(pc)Br.[22] However, the rotation angle of 40° between adjacent phthalocyanine rings in M(pc)I compunds remains unchanged in Ni(pc)Br. In short the metrical properties of M(pc)X are insensitive to the form of the counterion.

Despite the structural similarities, the conductivity and magnetic properties of Ni(pc)Br differ significantly from those of Ni(pc)I. The conductivity of the former increases upon cooling from room temperature, but then appears to level off by ca. 100 K, whereas that of the latter continues to increase down to at least 20 K, and remains high down to ~50 mK. Analysis of the carrier–spin *g* values suggests that the trihalide chain plays a lesser role in charge transport in Ni(pc)Br. More unusual, the analysis indicates that the Ni(pc) stacks become further decoupled as the temperature is lowered below ca. 75 K. The decoupling is accompanied by line width increases, which suggests that it reduces the mobility of the carrier spins. In contrast Ni(pc)I exhibits temperature-independent *g* values and the line width does not show the low-temperature increase seen in Figure 5 for Ni(pc)Br.

The physical basis for this decoupling and apparent loss of three-dimensional interaction in Ni(pc)Br will be characterized by low-temperature structural and NMR relaxation studies. However, the present results give the first clear evidence that it is inappropriate to ignore anion effects and concentrate on the metal–organic framework in discussions of the M(L)X systems.

Acknowledgment. This work was supported by the Northwestern University Materials Research Center under the National Science Foundation NSF-MRL program (Grant DMR 82-16972) and through the Solid State Chemistry Program of the National Science Foundation (Grant DMR 81-16804 to B.M.H.).

Registry No. Ni(pc), 14055-02-8; Br_2, 7726-95-6; Ni(pc)Br, 97187-14-9.

Supplementary Material Available: Table III, anisotropic thermal parameters (1 page). Ordering information is given on any current masthead page.

---

(19) Inabe, T.; Kannewurf, C. R.; Lyding, J. W.; Moguel, M. K.; Marks, T. J. *Mol. Cryst. Liq. Cryst.* **1983**, *93*, 355-367.

(20) DDQ = 2,3-dichloro-5,6-dicyano-1,4-benzoquinone; TNCQ = 7,7,8,8-tetracyano-*p*-quinodimethane.

(21) Euler, W. B. *Inorg. Chem.* **1984**, *23*, 2645-2650.

(22) Neither the Madelung energy (ref 21) nor the EHMO (ref 23) calculations account for the observed rotation angles.

(23) (a) Whangbo, M.-H.; Stewart, K. R. *Isr. J. Chem.* **1983**, *23*, 133-138. (b) Canadell, E.; Alvarez, S. *Inorg. Chem.* **1984**, *23*, 573-579.

Contribution from the Department of Chemistry, University of New Orleans, New Orleans, Louisiana 70148,
and Laboratoire de Spectrochimie des Elements de Transition, Université de Paris-Sud, 91405 Orsay, France

Binuclear Molecules Incorporating Small Molecules as Bridging Ligands. Magnetic Properties and Molecular Structure of $[Cu_2L(\mu\text{-}B)]^{2+}$ Where B = OH^- or Br^- and HL = 2,6-Bis(*N*-(2-pyridylmethyl)formidoyl)-4-methylphenol

Charles J. O'Connor,*[1a,b] Dale Firmin,[1a] Arun K. Pant,[1a,2] B. Ram Babu,[1a] and Edwin D. Stevens[1a]

Received January 15, 1986

The syntheses, crystal structures, and magnetic properties are reported for a series of copper(II) complexes prepared from a five-coordinate binucleating ligand, L^-, where HL = 2,6-bis(*N*-(2-pyridylmethyl)formidoyl)-4-methylphenol. These complexes incorporate different small exogenous ions (B^-) into a bridging position to form copper(II) *binuclear* complexes of the formula $[Cu_2L(B)]^{2+}$, and the various degrees of antiferromagnetic coupling are reported. Crystal data: $[Cu_2L(OH)](ClO_4)_2$, monoclinic, space group $P2_1/n$, $Z = 4$, $a = 21.167$ (4) Å, $b = 8.836$ (4) Å, $c = 13.834$ (3) Å, $\beta = 109.22$ (2)°, $V = 2443$ Å^3, $R = 3.3\%$ for 3723 reflections; $[Cu_2L(Br)]Br_2$, triclinic, space group $P\bar{1}$, $Z = 2$, $a = 7.601$ (7) Å, $b = 11.456$ (4) Å, $c = 13.266$ (8) Å, $\alpha = 77.10$ (4)°, $\beta = 83.88$ (6)°, $\gamma = 76.67$ (4)°, $V = 1094$ Å^3, $R = 5.9\%$ for 2544 reflections; $[Cu_2L(OH)](NO_3)_2 \cdot H_2O$, monoclinic, space group Pn, $Z = 2$, $a = 7.438$ (2) Å, $b = 14.823$ (2) Å, $c = 10.399$ (4) Å, $\beta = 90.23$ (2)°, $V = 1147$ Å^3, $R = 2.5\%$ for 2024 reflections.

Introduction

Magnetic interactions in binuclear complexes continue to be an area of research actively pursued by many laboratories. Over the past few years, the emphasis has shifted from the purely magnetic interest in exchange coupling to magnetostructural correlations in exchange-coupled systems.[3,4] From the literature of magnetochemical studies of binuclear complexes, it has become evident that metal complexes prepared from binucleating ligands

---

(1) (a) University of New Orleans. (b) Université de Paris-Sud.

(2) Permanent address: Department of Physics, University of Gorakhpur, Gorakhpur 273001, India.

(3) Willette, R. D., Gatteschi, D., Kahn, O., Eds. *Magneto-Structural Correlations in Exchange Coupled Systems*; D. Reidel: Dordrecht, Holland, 1984.

(4) O'Connor, C. J. *Prog. Inorg. Chem.* **1982**, *29*, 203.

0020-1669/86/1325-2300$01.50/0

allow the experimentalist more control over the structural factors that determine magnetic and electronic exchange properties. This synthetic advantage, when compared to the apparent random clustering that occurs in the more traditional dimeric systems, has resulted in a great deal of interest in the synthesis and characterization of the molecular and electronic structures of metal complexes derived from binucleating ligands.

The pioneering work of Robson and co-workers[5] introduced 2-formyl-4-methylsalicylaldehyde (**1**) as a building block for macrocyclic and nonmacrocyclic binucleating ligands. With this starting material, Robson prepared several macrocycles capable of surrounding two copper(II) ions. Some similar binuclear complexes based on the triketones have also been prepared by Lintvedt and co-workers[6] and found to have interesting electrochemical as well as magnetochemical properties. Gagné and co-workers have reexamined the electrochemical properties of several complexes derived from **1** and observed some mixed-valent Cu^{II}–Cu^{I} species from cyclic voltammetric scans.[7] These species were subsequently isolated and characterized. From the work of these and other investigators who will be discussed later, binuclear complexes derived from **1** were generally found to be antiferromagnetically coupled.

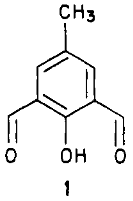

1

Following the initial work of Robson, interest in these types of complexes accelerated when it became evident that new species of coordinatively unsaturated binuclear molecules could be designed from **1** and its analogues. Much of the interest arose from the ability of these molecules to act as models for several interesting metalloproteins. In particular, there have been several attempts to model the active site of hemocyanin, a binuclear Cu^{II} oxygen carrier found in the hemolymph of some arthropods and mollusks.[8] An important criterion to be met by a good hemocyanin model is the ability to exhibit strong antiferromagnetic interactions over relatively long distances (3–5 Å). This condition is necessitated by the observation that oxyhemocyanin is found to exhibit strong antiferromagnetic coupling between two Cu^{II} centers,[9] linked through an exogenous peroxo bridge. The strong magnetic exchange phenomenon that is observed in oxyhemocyanin is not that unusual for metallobiomolecules that contain paramagnetic metals. In fact, magnetic exchange has also been observed in several metalloproteins that are involved in oxygen reduction and electron transport.[4,10]

The model complexes that researchers have designed to mimic metalloproteins are in general characterized by a coordinatively unsaturated binucleating ligand. When these binucleating ligands are coordinated to divalent transition metals (especially Cu^{II}), the resulting binuclear molecules are capable of accepting an exogenous ligand into a bridging coordination position.

The literature contains several reports of magnetic measurements on many macrocyclic as well as nonmacrocyclic binuclear compounds prepared from binucleating ligands synthesized from **1**. The reports include the original work by Robson[5] as well as more recent reports by Okawa and Kida,[11] Urbach,[12] Suzuki,[13] Mazurak,[14] Sorrell,[15,17] Kahn,[17,18] and O'Connor.[15–19] In general, these complexes show antiferromagnetic coupling; however, paramagnetic species have been observed by us[15] as well as other laboratories.[12,20] Our preliminary report[19] on this complex system contained the synthesis and magnetism of a Cu^{II} chloride binuclear complex resulting from the condensation of 2-(aminomethyl)pyridine with 2-formyl-4-methylsalicylaldehyde (**1**), producing the binucleating ligand 2,6-bis(*N*-(2-pyridylmethyl)formidoyl)-4-methylphenol (**2**), referred to in this report as HL. We have continued our study of the complexes of **2** with different exogenous bridging ligands (B). The general structure of the binuclear ionic complex that we are studying is shown as **3**. Included in our earlier report is a powder magnetic study of a slightly impure μ-hydroxide complex. After originally being able to obtain only powders, we

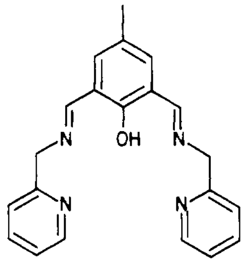

2

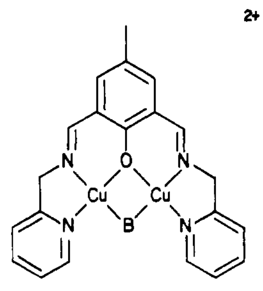

3

---

(5) Robson, R. *Inorg. Nucl. Chem. Lett.* **1970**, *6*, 125. Robson, R. *Aust. J. Chem.* **1970**, *23*, 2217. Pilkington, N. H.; Robson, R. *Aust. J. Chem.* **1970**, *23*, 2225. Hoskins, B. F.; Robson, R.; Schaap, H. *Inorg. Nucl. Chem. Lett.* **1972**, *8*, 21. McFayden, W. D.; Robson, R.; Schaap, H. *Inorg. Chem.* **1973**, *11*, 1777. Hoskins, B. F.; Robson, R.; Vice, D. *J. Chem. Soc., Chem. Commun.* **1973**, 392. Dickson, I. E.; Robson, R. *Inorg. Chem.* **1974**, *13*, 1301. Hoskins, B. F.; Robson, R.; Williams, G. A. *Inorg. Chim. Acta* **1976**, *16*, 121. McFayden, W. D.; Robson, R. *J. Coord. Chem.* **1976**, *5*, 49.

(6) Lintvedt, R. L.; Glick, M. D.; Tomlonovic, B. K.; Gavel, D. P.; Kuszaj, J. M. *Inorg. Chem.* **1976**, *15*, 1633. Fenton, D. E.; Schroeder, R. R.; Lintvedt, R. L. *J. Am. Chem. Soc.* **1978**, *100*, 1931. Fenton, D. E.; Lintvedt, R. L. *J. Am. Chem. Soc.* **1978**, *100*, 6367.

(7) Gagné, R. R.; Koval, C. A.; Smith, T. J. *J. Am. Chem. Soc.* **1977**, *99*, 8367. Gagné, R. R.; Kreh, R. P.; Kokge, J. A. *J. Am. Chem. Soc.* **1979**, *101*, 6917. Gagné, R. R.; Spiro, C. L.; Smith, T. J.; Hamaan, C. A.; Thies, W. R.; Shiekme, A. K. *J. Am. Chem. Soc.* **1981**, *103*, 4073. Smith, T. J.; Duesler, E. N.; Gagné, R. R.; Hendrickson, D. N. *Inorg. Chem.* **1981**, *20*, 1229.

(8) Lonti, R. *Structure and Function of Hemocyanin*; Bannister, J. V., Ed.; Springer-Verlag: Berlin, 1977; p 150. Solomon, E. I. In *Copper Proteins*; Spiro, T. G., Ed.; Wiley: New York, 1981; Chapter 1.

(9) Dooly, D. M.; Scott, R. A.; Ellinhaus, J.; Solomon, E. I.; Gray, H. B. *Proc. Natl. Acad. Sci. U.S.A.* **1978**, *75*, 3019.

(10) Tweedle, M. F.; Wilson, L. J.; Iniques, L. G.; Babcock, G. T.; Palmer, G. E. *J. Biol. Chem.* **1978**, *253*, 8065. Dawson, J. W.; Gray, H. B.; Hoenig, H. E.; Rossman, G. R.; Schreddar, J. M.; Wang, R.-H. *Biochemistry* **1972**, *11*, 461. Peterson, L.; Angstrom, J.; Ehrenberg, A. *Biochim. Biophys. Acta* **1978**, *526*, 211. Peterson, L.; Commack, R.; Rao, K. K. *Biochim. Biophys. Acta* **1980**, *622*, 19. Palmer, G.; Dunham, W. R.; Fee, J. A.; Sands, R. H.; Iizuka, T.; Yonetani, T. *Biochim. Biophys. Acta* **1971**, *201*, 2345. Moss, T. H.; Petering, D.; Palmer, G. *J. Biol. Chem.* **1969**, *244*, 2275.

(11) Okawa, H.; Tokii, T.; Nonaka, Y.; Nuto, Y.; Kida, S. *Bull. Chem. Soc. Jpn.* **1973**, *46*, 1462. Okawa, H.; Tokii, T.; Muto, Y.; Kida, S. *Bull. Chem. Soc. Jpn.* **1973**, *46*, 2464. Okawa, H.; Ando, I.; Kida, S. *Bull. Chem. Soc. Jpn.* **1974**, *47*, 3041. Ichinose, T.; Nishida, Y.; Okawa, H.; Kida, S. *Bull. Chem. Soc. Jpn.* **1974**, *47*, 3045. Okawa, H. *Bull. Chem. Soc. Jpn.* **1970**, *43*, 3019. Okawa, H.; Kida, S. *Bull. Chem. Soc. Jpn.* **1971**, *44*, 1172. Okawa, H.; Kida, S. *Bull Chem. Soc. Jpn.* **1972**, *45*, 1759. Okawa, H.; Kida, S.; Mota, Y.; Tokii, T. *Bull. Chem. Soc. Jpn.* **1972**, *45*, 2480. Okawa, H.; Honda, M.; Kida, S. *Chem. Lett.* **1972**, 1027.

(12) Grzybowski, J. J.; Merrell, P. H.; Urbach, F. L. *Inorg. Chem.* **1978**, *17*, 3078. Grzybowski, J. J.; Urbach, F. L. *Inorg. Chem.* **1980**, *19*, 2604. Urbach, F. L. *Met. Ions Biol. Syst.* **1981**, *13*, 73.

(13) Suzuki, M.; Kanatomi, H.; Demura, Y.; Miurase, I. *Bull. Chem. Soc. Jpn.* **1984**, *57*, 1003.

(14) Mazurak, W.; Kennedy, B. J.; Murray, K. S.; O'Connor, M. J.; Rodgers, J. R.; Snow, M. R.; Wedd, A. G.; Zwak, P. R. *Inorg. Chem.* **1985**, *24*, 3258.

(15) Sorrell, T. N.; Jameson, D. L.; O'Connor, C. J. *Inorg. Chem.* **1984**, *23*, 190.

(16) Sorrell, T. N.; O'Connor, C. J.; Anderson, O. P.; Reibenspeis, J. *J. Am. Chem. Soc.* **1985**, *107*, 4199.

(17) O'Connor, C. J.; Sorrell, T. N.; Kahn, O. *J. Magn. Magn. Mater.* **1986**, *54–57*, 1478.

(18) Boillot, M. L.; Kahn, O.; O'Connor, C. J.; Gouteron, J.; Jeannin, S.; Jeannin, Y. *J. Chem. Soc., Chem. Commun.* **1985**, 178.

(19) Eduok, E. E.; O'Connor, C. J. *Inorg. Chim. Acta* **1984**, *88*, 229.

(20) McKee, V.; Dadigian, J. V.; Bau, R.; Reed, C. A. *J. Am. Chem. Soc.* **1981**, *103*, 7000. McKee, V.; Zvagulius, M.; Dadigian, J. V.; Patch, M. G.; Reed, C. A. *J. Am. Chem. Soc.* **1984**, *106*, 4765.

hav now isolated single crystals of 3 with B = OH^- and X = ClO_4^-. We report here a detailed analysis of the structure and magnetism of the complexes of 3 with B = OH^- and X = ClO_4^- and NO_3^- and with B = Br^- and X = Br^-. Each of these complexes is antiferromagnetically coupled, with coupling parameters ranging from $2J = -499$ cm^{-1} (OH^-) to $2J = -68$ cm^{-1} (Br^-).

Experimental Section

Syntheses. 2-Formyl-4-methylsalicylaldehyde (1). The dialdehyde 2-formyl-4-methylsalicylaldehyde was prepared by the method of Ullman and Brittner.[21]

2,6-Bis(*N*-(2-pyridylmethyl)formidoyl)-4-methylphenol (2, HL). Stoichiometric quantities of the dialdehyde prepared as described above and 2-(aminomethyl)pyridine were dissolved in a minimum amount of anhydrous methanol and then mixed together. The reaction occurred without heating and resulted in a yellow solution. This solution was used for subsequent reactions without further purification.

$[Cu_2L(OH)](ClO_4)_2$ (A). Stochiometric amounts of HL in methanol and copper(II) perchlorate in methanol were mixed, resulting in a dark green solution. The solution evaporated slowly in a desiccator; however, the resulting crystals were not suitable for X-ray analysis. The material was redissolved in 50:50 ethanol/acetonitrile solution and again allowed to slowly evaporate in a sulfuric acid desiccator. This time large well-developed dark colored crystals were obtained.

$[Cu_2L(Br)]Br_2$ (B). A stoichiometric quantity of copper(II) bromide was dissolved in methanol and allowed to react with the methanolic solution of HL. The solution immediately turned a dark green and formed some precipitate. The solution was allowed to evaporate slowly in a sulfuric acid desiccator for 2 days. Filtration of this solution gave a large quantity of shiny brown crystals plus a few dark blue crystals of impurity. The solid was recrystallized in methanol to form a green solution. An equal volume of acetonitrile was added, forming a dark green-brown solution. After 4 days of slow evaporation in a sulfuric acid desiccator, dark colored crystals were filtered, washed with absolute ethanol, and dried under nitrogen.

$[Cu_2L(OH)](NO_3)_2{\cdot}H_2O$ (C). Stoichiometric amounts of HL in methanol and copper(II) nitrate in hot methanol were mixed, resulting in a dark green solution. This solution was placed in a sulfuric acid desiccator for 2 days and evaporated to half-volume. The solution was then filtered, yielding flat blue-green crystals that were washed in methanol and dried.

Magnetism. The magnetic susceptibilities of the complexes were measured over the 6–400 K temperature region with a superconducting SQUID susceptometer. Measurement and calibration procedures are reported elsewhere.[4] The data are included in the supplementary material.

X-ray Procedures. Collection and Reduction of Intensity Data. A summary of crystal and intensity data and refinement of structures of $[Cu_2L(OH)](ClO_4)_2$ (hereinafter referred to as A), $[Cu_2L(Br)]Br_2$ (hereinafter referred to as B), and $[Cu_2L(OH)](NO_3)_2{\cdot}H_2O$ (hereinafter referred to as C) is given in Table I.

For each of the compounds intensity data were collected on Enraf-Nonius CAD-4 four-circle diffractometer in the ω–2θ scan mode. Scan widths were determined from the formula $SW = A + B \tan \theta$, where A takes care of the mosaic nature of the crystal and B allows for the increase in peak width due to $K\alpha_1 - K\alpha_2$ splitting. The calculated scan angle is extended at each side by SW/4 for background measurements (BG1 and BG2). The net count is then calculated as $I_{NC} = I_{2/3} - 2(BG1 + BG2)$ where $I_{2/3}$ is the integrated peak intensity of the central two-thirds portion of the peak. In each case, (i) the crystal orientation was checked after every 200 reflections and (ii) three standard reflections were monitored every two hours. Intensities were corrected for Lorentz–polarization and background effects. Empirical absorption corrections were applied on the basis of ψ-scan data. No attempts were made to correct the intensities for fine absorption. No decay and extinction corrections were found necessary.

Solution and Refinement of Structures. The structures of all the complexes, A, B, and C, were solved by direct methods using the program MULTAN 80.[22] Successive Fourier and difference syntheses alternated with full-matrix least-squares refinement revealed the positions of all the atoms including the hydrogen atoms for A and C. The structures A and C were finally refined with anisotropic thermal parameters for non-hydrogen atoms and isotropic thermal parameters for hydrogen atoms.

For complex B the 19 hydrogen atoms were added in calculated positions once the refinement for non-hydrogen atoms had converged and were assigned thermal parameters equal to the isotropic equivalents of the parent atoms. With the hydrogen positional and thermal parameters remaining fixed, a few more full-matrix least-squares cycles brought the R value down from 0.061 (without hydrogens) to 0.059. The hydrogen atom positions of the CH_3 group could still be uncertain although a difference map plotted after the refinement had fully converged did not reveal anything. For atoms O1, C6, and C8 the thermal parameters became nonpositive definite. This is perhaps partly due to the large value of the linear absorption coefficient ($\mu = 74$ cm^{-1}) and partly due to the relatively poor quality of the crystal: the value of 1.8 used for the scan width parameter "A" is indicative of the broad mosaic distribution.[23,24] In all the calculations atomic scattering factors were taken from ref 25.

Results and Discussion

The final positional parameters for binuclear Cu^{II} complexes A, B, and C are listed in Table IIa–c. Main distances and angles involving non-hydrogen atoms are given in Tables III and IV, respectively. Parts a–c of Figure 1 show perspective views of the molecules together with the numbering schemes.

The main ligand in these binuclear complexes is pentadentate. The bond lengths and angles within the ligand are generally very similar in all the cases and are also comparable to those in another binuclear Cu^{II} complex, $Cu_2(C_{21}H_{19}N_4O)Cl_3{\cdot}H_2O$, having the same ligand.[26] The main ligand is more nearly planar for A and C than for B, the atom deviations lying between −0.198 and +0.274 Å for A, −0.418 and +0.388 Å for B, and −0.167 and +0.130 Å for C. For pyridine and phenyl ring planes, the dihedral angles with the least-squares planes of the main ligand are 6.3, 8.3, and 3.4° for A, 8.7, 17.4, and 3.4° for B, and 6.6, 3.8, and 2.7° for C. The dihedral angles between the two planes defined by Cu1 and the two briding atoms and Cu2 and the same two bridging atoms are respectively 16, 33.5, and 10° for A, B, and C, again showing the large deviation from planarity in complex B.

Some of the distances for A, B, and C, respectively Cu–N(imine) [average 1.921 (2), 1.957 (7), and 1.923 (3) Å], Cu–N(py) [average 1.964 (2), 1.997 (8), and 1.991 (5) Å], Cu–O1(bridging) [average 1.936 (1), 1.970 (6), and 1.954 (3) Å], and Cu1–Cu2 [2.947 (0), 3.151 (2), and 2.991 (1) Å], are significantly different but follow similar trends. The variations are probably due to the differences in the small molecules used as bridging ligands.

The coordination around Cu and the molecular packing, which are quite different in the three complexes, are discussed separately.

$[Cu_2L(OH)](ClO_4)_2$. Each Cu^{II} ion is coordinated to two N atoms, and both Cu^{II} ions are coordinated to the phenolic oxygen, O1, forming an O atom bridge, and are also bridged through another oxygen, O2, of the hydroxide ion. In addition, both the Cu^{II} ions are also coordinated to oxygen atoms O8 and O10 of the *same* perchlorate ion (making it bidentate), the distances being Cu1–O10 = 2.450 (1) Å and Cu2–O8 = 2.587 (1) Å, forming a bridge Cu1–O10–Cl2–O8–Cu2. Each Cu^{II} ion is thus pentacoordinate. The other perchlorate ion is moderately well separated and is weakly bound by several O···O van der Waals contacts—the shortest being O6···C3 = 3.229 (3) Å. Both the perchlorate ions have nearly perfect tetrahedral geometry, the Cl–O bond length and O–Cl–O bond angle spreads being respectively 1.422–1.456 (2) Å (average 1.438 Å) and 108.9–110.6 (1)° (average 109.46°) for the nonbridging and 1.424–1.453 (2) Å (average 1.437 Å) and 109.0–111.0 (1)° (average 109.48°) for the bridging perchlorate. Both the perchlorate ions show large vibrational amplitudes of motion, as can be seen from the higher temperature factors of the O atoms. A similar bridging perchlorate ion has earlier been

---

(21) Ullmann, F.; Brittner, K. *Ber. Dtsch. Chem. Ges.* **1909**, 2539.

(22) Main, P.; Fiske, S. J.; Hull, S. E.; Lessinger, L.; Germaine, G.; Declerg, J.-P.; Woolfson, M. M. *MULTAN80. A System of Computer Programs for the Automatic Solution of Crystal Structures from X-ray Diffraction Data*; Universities of York and Louvain: England, Belgium, 1980.

(23) The calculations were performed on a PDP 11/34 computer using the CAD4 SDP program system.

(24) Frenz, B. *SDP Package of Computer Programs*; Makenlar Structure Corp.: College Station, TX, 1982.

(25) *International Tables for X-ray Crystallography*; Kynoch: Birmingham, England, 1974; Vol. IV.

(26) Majeste, R. J.; Klein, C. L.; Stevens, E. D. *Acta Crystallogr., Sect. C: Cryst. Struct. Commun.* **1983**, *C39*, 52.

Table I. Summary of Crystal Data, Collection and Reduction of X-ray Data, and Solution and Refinement of Structures

	$[Cu_2L(OH)](ClO_4)_2$ (A)	$[Cu_2L(Br)]Br_2$ (B)	$[Cu_2L(OH)]$-$(NO_3)_2 \cdot H_2O$ (C)
(a) Crystal Data			
cryst color	blackish green	blackish brown	greenish blue
cryst shape	rhombohedral	parallelepiped	platelike
cryst dimens, mm^3	0.6 × 0.5 × 0.3	0.3 × 0.2 × 0.2	0.35 × 0.25 × 0.1
cryst syst	monoclinic	triclinic	monoclinic
space group	$P2_1/n$	$P\bar{1}$	Pn
syst absences	$h0l$ for $h + l = 2n + 1$ $0k0$ for $k = 2n + 1$	none	$h0l$ for $h + l = 2n + 1$
temp, K	125	100	90
cell params (errors)^a			
a, Å	21.167 (4)	7.601 (7)	7.438 (2)
b, Å	8.836 (4)	11.456 (4)	14.823 (2)
c, Å	13.834 (3)	13.266 (8)	10.399 (4)
α, deg	90	77.10 (4)	90
β, deg	109.22 (2)	83.88 (6)	90.23 (2)
γ, deg	90	76.67 (4)	90
V, Å^3	2443	1094	1147
Z	4	2	2
fw	686	710	630
calcd density, g cm^{-3}	1.863	2.157	1.823
measd density (flotation), g cm^{-3}	1.864		
abs coeff (Mo Kα), cm^{-1}	20.3	74.0	18.6
(b) Collection and Reduction of X-ray Diffraction Data			
diffractometer	CAD4	CAD4	CAD4
radiation (graphite-monochromated)	Mo Kα	Mo Kα	Mo Kα
wavelength, Å	0.7107	0.7107	0.7107
scan type	ω–2θ	ω–2θ	ω–2θ
2θ limits, deg	2–50	2–50	2–50
no. of reflcns measd	4620	3527	2303
cutoff of obsd data	$3\sigma(I)$	$3\sigma(I)$	$3\sigma(I)$
no. of obsd reflcns	3723	2544	2024
scan width params			
A	0.9	1.8	1.0
B	0.35	0.35	0.35
abs cor method	ψ scans	ψ scans	ψ scans
transmissn coeff limits	0.91–0.99	0.60–0.99	0.92–1.00
(c) Solution and Refinement			
technique of soln	direct methods with MULTAN	direct methods with MULTAN	direct methods with MULTAN
method of refinement	full-matrix LS^b	full-matrix LS^b	full-matrix LS^b
no. of variables	432	280	416
R^c	0.033	0.059	0.025
R_w	0.044	0.081	0.033
GOF	2.672	1.691	1.286
P	0.03	0.01	0.04
max shift (Δ/σ)	<0.01	0.03	0.01

[a] Cell dimensions and their esd's were obtained from least-squares refinement of 25 accurately centered reflections having θ's around 25°. [b] The function minimized is $\sum w(F_o - F_c)^2$, where $w = 1/\sigma_F^2 = 4F^2/(\sigma_F^2)^2$, $(\sigma_F^2)^2 = \sigma_I^2 + (PF^2)^2$, and σ_I and P are respectively the standard deviation on I based on counting statistics and the experimental instability factor used to downweight intense reflections. [c] The unweighted and weighted residuals are defined as $R = \sum||F_o| - |F_c||/\sum|F_o|$ and $R_w = [\sum w(|F_o| - |F_c|)^2/(\sum w|F_o|^2)]^{1/2}$. The error in an observation of unit weight (GOF) is $[\sum w(|F_o| - |F_c|)^2/(NO - NV)]^{1/2}$, where NO and NV are the numbers of observations and variables, respectively.

reported in $[Cu_3OHL_3(ClO_4)]ClO_4$,[27] where however the bond length [1.252 (11)–1.460 (5) Å] and bond angle [95.5 (1)–115.5 (5)°] spreads are much larger although the Cu–O distances are quite similar [2.428 (6) and 2.552 (9) Å].

Each Cu^{II} ion has a very slightly distorted square-pyramidal coordination, the distortion from square planar toward trigonal-bipyramidal conformation being more for Cu2. The Cu–O(H) bridging distances of 1.915 (1) and 1.920 (1) Å in complex A are comparable to those of 1.930 (5) and 1.930 (5) Å in the binuclear Cu^{II} complex $[(bpy)_2Cu\text{–}OH\text{–}Cu(bpy)_2](ClO_4)_3$,[28] where bpy is 2,2′-bipyridine, but are significantly shorter than those of 1.946 (6), 1.969 (4) and 1.979 (6) Å found in the trinuclear Cu^{II} complex $[Cu_3OHL_3(ClO_4)]ClO_4$,[27] where LH = 3-(phenylimino)butanone 2-oxime.

The packing of the molecules is dictated mainly by van der Waals interactions. There are no unusually short intermolecular distances.

$[Cu_2L(Br)]Br_2$. Each Cu^{II} ion is coordinated to two N atoms, and both of the Cu^{II} ions are coordinated to the phenolic oxygen, O1, forming an O atom bridge. They are also bridged through a bromine atom, Br3. In addition, Cu1 and Cu2 are coordinated to Br1 and Br2, respectively, making them pentacoordinate with distorted square-pyramid geometries. The nonbridging Br atoms are coordinated on opposite sides of the molecule. It is interesting to note that whereas for Cu1 the Cu1–Br3(bridging) and Cu1–Br1(nonbridging) lengths are 2.707 (2) and 2.413 (2) Å, respectively, for Cu2 these are in reverse order: Cu2–Br3(bridging) = 2.426 (2) Å and Cu2–Br2(nonbridging) = 2.719 (2) Å. In the case of the corresponding chloro compound,[26] the Cu–Cl(bridging) [2.309 (2) and 2.297 (2) Å] and Cu–Cl(nonbridging) [2.523 (2) and 2.524 (2) Å] lengths are very similar. The relatively larger size of the bromine atoms is probably responsible for the difference.

The packing of the molecules is mainly due to van der Waals interactions as opposed to that in the corresponding chloro compound,[26] which had two water molecules of hydration in a unit cell, resulting in an intermolecular hydrogen bond network.

---

(27) Butcher, R. J.; O'Connor, C. J.; Sinn, E. *Inorg. Chem.* **1981**, *20*, 537.
(28) Haddad, M. S.; Wilson, S. R.; Hodgson, D. J.; Hendrickson, D. N. *J. Am. Chem. Soc.* **1981**, *103*, 384.

Table II. Table of Positional Parameters and Their Estimated Standard Deviations[a]

(a) $[Cu_2L(OH)](ClO_4)_2$ (Complex A)

atom	*x*	*y*	*z*	*B*, Å^2	atom	*x*	*y*	*z*	*B*, Å^2
Cu1	0.50827 (2)	0.39003 (4)	0.89070 (2)	1.118 (7)	C13	0.4135 (1)	0.4848 (3)	0.6880 (2)	1.28 (6)
Cu2	0.55567 (2)	0.58331 (4)	0.75501 (2)	1.203 (7)	C14	0.4500 (2)	0.6481 (4)	0.5668 (2)	1.65 (6)
Cl1	0.24046 (3)	0.48540 (9)	0.91077 (5)	1.55 (1)	C15	0.5558 (2)	0.7534 (4)	0.5792 (2)	1.86 (6)
Cl2	0.55822 (3)	0.18380 (8)	0.71934 (5)	1.55 (1)	C16	0.6266 (2)	0.7399 (3)	0.6481 (2)	1.55 (6)
O1	0.47371 (9)	0.4927 (2)	0.7600 (1)	1.34 (4)	C17	0.6795 (2)	0.7938 (4)	0.6207 (2)	1.92 (6)
O2	0.58219 (9)	0.5187 (2)	0.8949 (1)	1.33 (4)	C18	0.7436 (2)	0.7751 (4)	0.6873 (2)	1.94 (6)
O3	0.2822 (1)	0.5811 (2)	0.9926 (2)	1.61 (4)	C19	0.7544 (2)	0.7045 (4)	0.7810 (2)	1.96 (6)
O4	0.2661 (1)	0.3338 (3)	0.9261 (2)	2.60 (5)	C20	0.6992 (2)	0.6549 (4)	0.8040 (2)	1.64 (6)
O5	0.2431 (1)	0.5403 (3)	0.8141 (2)	3.18 (6)	C21	0.2133 (2)	0.4860 (4)	0.4634 (3)	2.09 (7)
O6	0.1736 (1)	0.4896 (4)	0.9124 (2)	4.18 (6)	H(O2)	0.613 (2)	0.499 (4)	0.912 (2)	2.3 (7)*
O7	0.5984 (1)	0.0629 (3)	0.7040 (2)	3.13 (5)	H1	0.630 (1)	0.363 (3)	1.084 (2)	0.5 (6)*
O8	0.5802 (1)	0.3250 (3)	0.6869 (2)	2.32 (5)	H2	0.652 (2)	0.216 (4)	1.231 (2)	2.7 (8)*
O9	0.4893 (1)	0.1594 (3)	0.6627 (2)	3.11 (6)	H3	0.571 (2)	0.073 (4)	1.263 (2)	2.0 (7)*
O10	0.5661 (1)	0.1935 (2)	0.8270 (2)	1.77 (4)	H4	0.465 (2)	0.062 (4)	1.144 (3)	2.5 (8)*
N1	0.5361 (1)	0.2889 (3)	1.0251 (2)	1.27 (5)	H6(1)	0.386 (1)	0.236 (3)	0.982 (2)	0.7 (6)*
N2	0.4230 (1)	0.2975 (3)	0.8727 (2)	1.23 (5)	H6(2)	0.410 (1)	0.100 (3)	0.933 (2)	1.1 (6)*
N3	0.5118 (1)	0.6647 (3)	0.6208 (2)	1.50 (5)	H7	0.332 (1)	0.263 (3)	0.799 (2)	0.6 (6)*
N4	0.6366 (1)	0.6704 (3)	0.7389 (2)	1.39 (5)	H9	0.264 (1)	0.345 (3)	0.642 (2)	1.2 (6)*
C1	0.5972 (1)	0.2932 (4)	1.0978 (2)	1.56 (6)	H11	0.330 (1)	0.612 (3)	0.461 (2)	1.1 (6)*
C2	0.6118 (2)	0.2130 (4)	1.1879 (2)	1.80 (6)	H14	0.437 (2)	0.691 (5)	0.506 (3)	4 (1)*
C3	0.5621 (2)	0.1270 (4)	1.2047 (2)	1.93 (6)	H15(1)	0.543 (2)	0.839 (4)	0.579 (3)	2.9 (8)*
C4	0.4993 (2)	0.1223 (3)	1.1312 (2)	1.74 (6)	H15(2)	0.550 (2)	0.719 (4)	0.513 (2)	2.0 (7)*
C5	0.4876 (1)	0.2042 (3)	1.0414 (2)	1.31 (6)	H17	0.674 (2)	0.837 (4)	0.569 (2)	2.5 (8)*
C6	0.4209 (1)	0.2031 (3)	0.9586 (2)	1.40 (6)	H18	0.781 (1)	0.801 (3)	0.671 (2)	1.3 (6)*
C7	0.3691 (1)	0.3113 (3)	0.7949 (2)	1.35 (6)	H19	0.796 (1)	0.684 (3)	0.831 (2)	0.8 (6)*
C8	0.3613 (1)	0.4004 (3)	0.7042 (2)	1.43 (6)	H20	0.703 (2)	0.607 (4)	0.861 (3)	2.8 (8)*
C9	0.2981 (2)	0.4025 (3)	0.6305 (2)	1.57 (6)	H21(1)	0.192 (2)	0.403 (4)	0.477 (3)	3.5 (9)*
C10	0.2831 (1)	0.4817 (4)	0.5389 (2)	1.57 (6)	H21(2)	0.217 (2)	0.488 (5)	0.406 (3)	5 (1)*
C11	0.3356 (2)	0.5592 (4)	0.5229 (2)	1.72 (6)	H21(3)	0.190 (2)	0.570 (4)	0.476 (3)	3.6 (9)*
C12	0.4004 (1)	0.5626 (3)	0.5944 (2)	1.50 (6)					

(b) $[Cu_2L(Br)]Br_2$ (Complex B)

atom	*x*	*y*	*z*	*B*, Å^2	atom	*x*	*y*	*z*	*B*, Å^2
Br1	−0.0061 (2)	0.3543 (1)	0.85058 (8)	1.74 (2)	C7	0.243 (1)	−0.060 (1)	0.9967 (8)	1.3 (2)
Br2	0.6680 (2)	0.0967 (1)	0.59676 (9)	1.85 (2)	C8	0.210 (1)	−0.079 (1)	0.8954 (7)	1.2 (2)
Br3	0.5087 (2)	0.29729 (9)	0.79934 (8)	1.45 (2)	C9	0.175 (2)	−0.191 (1)	0.8909 (8)	1.7 (2)
Cu1	0.2474 (2)	0.1962 (1)	0.91758 (9)	1.30 (3)	C10	0.138 (2)	−0.222 (1)	0.8007 (8)	1.4 (2)
Cu2	0.3610 (2)	0.2248 (1)	0.6793 (1)	1.39 (3)	C11	0.139 (2)	−0.131 (1)	0.7100 (8)	1.5 (2)
O1	0.273 (1)	0.1129 (6)	0.8025 (5)	1.3 (2)	C12	0.177 (1)	−0.0181 (9)	0.7061 (8)	1.1 (2)
N1	0.295 (1)	0.2525 (7)	1.0405 (7)	1.3 (2)	C13	0.221 (1)	0.0115 (9)	0.8021 (7)	1.0 (2)
N2	0.270 (1)	0.0397 (8)	1.0151 (6)	1.4 (2)	C14	0.168 (2)	0.069 (1)	0.6093 (8)	1.4 (2)
N3	0.224 (1)	0.1667 (7)	0.5897 (6)	1.3 (2)	C15	0.220 (2)	0.241 (1)	0.4841 (8)	1.7 (2)
N4	0.298 (1)	0.3811 (8)	0.5722 (7)	1.3 (2)	C16	0.232 (2)	0.368 (1)	0.4869 (8)	1.6 (2)
C1	0.323 (2)	0.366 (1)	1.0384 (9)	2.1 (3)	C17	0.182 (2)	0.468 (1)	0.4077 (9)	1.8 (2)
C2	0.375 (2)	0.397 (1)	1.1243 (9)	1.7 (2)	C18	0.192 (2)	0.582 (1)	0.415 (1)	2.0 (3)
C3	0.406 (2)	0.308 (1)	1.2141 (9)	1.6 (2)	C19	0.261 (2)	0.595 (1)	0.5065 (8)	1.5 (2)
C4	0.376 (2)	0.193 (1)	1.2184 (8)	1.8 (2)	C20	0.313 (2)	0.496 (1)	0.5806 (9)	1.8 (2)
C5	0.326 (2)	0.167 (1)	1.1267 (8)	1.3 (2)	C21	0.111 (2)	−0.348 (1)	0.7995 (9)	1.9 (3)
C6	0.290 (2)	0.0422 (9)	1.1228 (8)	1.4 (2)					

(c) $[Cu_2L(OH)](NO_3)_2 \cdot H_2O$ (Complex C)

atom	*x*	*y*	*z*	*B*, Å^2	atom	*x*	*y*	*z*	*B*, Å^2
Cu1	0.2533 (fixed)	0.24691 (4)	0.7237 (fixed)	1.223 (9)	C6	0.2411 (7)	0.0541 (3)	0.7054 (5)	1.70 (9)
					C7	−0.0029 (7)	0.1274 (3)	0.6024 (5)	1.38 (8)
Cu2	0.16356 (9)	0.43853 (4)	0.66004 (7)	1.259 (9)	C8	−0.1209 (7)	0.1988 (3)	0.5590 (5)	1.40 (9)
O1	0.0771 (4)	0.3187 (2)	0.6234 (3)	1.29 (6)	C9	−0.2829 (7)	0.1738 (3)	0.5045 (4)	1.50 (9)
O2	0.3506 (5)	0.3673 (2)	0.7357 (4)	1.65 (6)	C10	−0.4131 (7)	0.2354 (4)	0.4662 (5)	1.7 (1)
O3	−0.0157 (5)	0.4476 (3)	0.8863 (4)	1.89 (7)	C11	−0.3708 (6)	0.3255 (3)	0.4801 (4)	1.37 (8)
O4	−0.2278 (5)	0.5479 (3)	0.8927 (4)	2.25 (7)	C12	−0.2073 (7)	0.3556 (3)	0.5325 (4)	1.45 (9)
O5	−0.2885 (5)	0.4103 (3)	0.8344 (4)	2.14 (7)	C13	−0.0769 (7)	0.2920 (3)	0.5752 (4)	1.38 (9)
O6	0.0785 (5)	0.2641 (2)	0.8937 (4)	1.81 (6)*	C14	−0.1856 (7)	0.4527 (3)	0.5419 (4)	1.40 (9)
O7	−0.2534 (6)	−0.1938 (3)	0.6040 (4)	3.42 (9)	C15	−0.0459 (7)	0.5925 (3)	0.5908 (5)	1.53 (9)
O8	−0.3226 (6)	−0.0659 (3)	0.5143 (4)	3.02 (9)	C16	0.1340 (6)	0.6256 (3)	0.6376 (4)	1.36 (9)
O9	−0.0666 (5)	−0.0842 (3)	0.6118 (4)	2.77 (8)	C17	0.1783 (7)	0.7171 (3)	0.6400 (5)	1.74 (9)
N1	0.4532 (5)	0.1653 (3)	0.7813 (4)	1.28 (7)	C18	0.3452 (8)	0.7429 (4)	0.6846 (5)	2.0 (1)
N2	0.1447 (6)	0.1357 (3)	0.6654 (4)	1.34 (7)	C19	0.4629 (7)	0.6779 (4)	0.7264 (5)	1.9 (1)
N3	−0.0479 (5)	0.4939 (3)	0.5876 (4)	1.27 (7)	C20	0.4120 (7)	0.5897 (4)	0.7222 (5)	1.8 (1)
N4	0.2529 (5)	0.5635 (3)	0.6757 (4)	1.27 (7)	C21	−0.5881 (7)	0.2058 (4)	0.4079 (5)	2.1 (1)
N5	−0.1795 (6)	0.4698 (3)	0.8712 (4)	1.43 (7)	H1	0.627 (8)	0.222 (4)	0.835 (6)	1.89 (fixed)
N6	−0.2146 (6)	−0.1143 (3)	0.5763 (4)	1.89 (8)					
C1	0.6100 (8)	0.1896 (4)	0.8316 (5)	2.0 (1)	HO2	0.446 (7)	0.376 (4)	0.752 (5)	1.87 (fixed)
C2	0.7422 (6)	0.1286 (4)	0.8665 (5)	1.57 (9)					
C3	0.7078 (8)	0.0381 (4)	0.8436 (5)	2.0 (1)	H2	−0.145 (7)	0.145 (4)	0.895 (5)	1.55 (fixed)
C4	0.5472 (7)	0.0124 (4)	0.7916 (5)	1.81 (9)					
C5	0.4196 (7)	0.0775 (4)	0.7606 (5)	1.54 (9)	H3	0.799 (7)	−0.005 (4)	0.861 (5)	0.8 (9)*

Table II (Continued)

(c) $[Cu_2L(OH)](NO_3)_2{\cdot}H_2O$ (Complex C)

atom	x	y	z	B, Å^2	atom	x	y	z	B, Å^2
H4	0.504 (9)	−0.052 (4)	0.769 (7)	3 (1)*	H61	0.763 (8)	−0.008 (4)	1.150 (6)	3 (1)*
H7	0.460 (7)	−0.074 (3)	1.078 (5)	1 (1)*	H62	0.153 (9)	0.025 (5)	0.799 (7)	4 (2)*
H9	0.190 (6)	−0.120 (3)	0.994 (4)	0.2 (8)*	H151	0.444 (7)	0.389 (4)	1.007 (5)	1 (1)*
H11	0.561 (6)	0.366 (3)	0.457 (4)	0.3 (8)*	H152	0.369 (9)	0.383 (5)	0.149 (6)	3 (1)*
H14	−0.295 (6)	0.487 (3)	0.504 (4)	0.2 (8)*	H211	0.418 (7)	0.195 (4)	1.324 (5)	1 (1)*
H17	0.586 (8)	0.250 (3)	1.115 (6)	1 (1)*	H212	0.337 (9)	0.254 (4)	0.418 (7)	3 (1)*
H18	−0.10 (1)	0.191 (6)	1.173 (8)	6 (2)*	H213	0.368 (8)	0.161 (5)	0.445 (6)	3 (1)*
H19	0.063 (7)	0.311 (4)	1.245 (5)	1.87 (fixed)	HO62	0.12 (1)	0.234 (4)	0.980 (6)	3 (1)*
					HO61	0.041	0.334	0.916	4.00 (fixed)
H20	0.496 (9)	0.549 (4)	0.753 (6)	2 (1)*					

[a] Values marked with an asterisk indicate that the atoms were refined isotropically. Anisotropically refined atoms are given in the form of the isotropic equivalent thermal parameter defined as $^4/_3[a^2B(1,1) + b^2B(2,2) + c^2B(3,3) + ab(\cos\gamma)B(1,2) + ac(\cos\beta)B(1,3) + bc(\cos\alpha)B(2,3)]$.

Table III. Selected Interatomic Distances (Å)

atom 1	atom 2	dist	atom 1	atom 2	dist
		(a) $[Cu_2L(OH)](ClO_4)_2$ (Complex A)			
Cu1	Cu2	2.947 (0)	Cu2	N4	1.957 (2)
Cu1	O1	1.938 (1)	Cl1	O3	1.456 (1)
Cu1	O2	1.920 (1)	Cl1	O4	1.434 (2)
Cu1	O10	2.450 (1)	Cl1	O5	1.441 (2)
Cu1	N1	1.970 (2)	Cl1	O6	1.422 (2)
Cu1	N2	1.921 (2)	Cl2	O7	1.424 (2)
Cu2	O1	1.933 (1)	Cl2	O8	1.453 (1)
Cu2	O2	1.915 (1)	Cl2	O9	1.427 (2)
Cu2	O8	2.587 (1)	Cl2	O10	1.445 (1)
Cu2	N3	1.921 (2)			
		(b) $[Cu_2L(Br)]Br_2$ (Complex B)			
Cu1	Cu2	3.151 (2)	Cu2	Br2	2.719 (2)
Cu1	Br1	2.413 (2)	Cu2	Br3	2.426 (2)
Cu1	Br3	2.707 (2)	Cu2	O1	1.995 (6)
Cu1	O1	1.945 (6)	Cu2	N3	1.968 (8)
Cu1	N1	1.977 (8)	Cu2	N4	2.017 (8)
Cu1	N2	1.946 (7)			
		(c) $[Cu_2L(OH)](NO_3)_2{\cdot}H_2O$ (Complex C)			
Cu1	Cu2	2.992 (1)	Cu2	N3	1.925 (4)
Cu1	O1	1.981 (3)	Cu2	N4	1.975 (4)
Cu1	O2	1.930 (3)	O6	O7	2.722 (5)
Cu1	O6	2.213 (4)	O6	O3	2.809 (5)
Cu1	N1	2.006 (6)	N5	O3	1.271 (5)
Cu1	N2	1.933 (2)	N5	O4	1.233 (6)
Cu2	O1	1.927 (3)	N5	O5	1.256 (6)
Cu2	O2	1.913 (3)	N6	O7	1.248 (6)
Cu2	O3	2.712 (4)	N6	O8	1.253 (6)
Cu2	O4[a]	2.905 (4)	N6	O9	1.242 (6)

[a] $^1/_2 + x, 1 - y, -^1/_2 + z$.

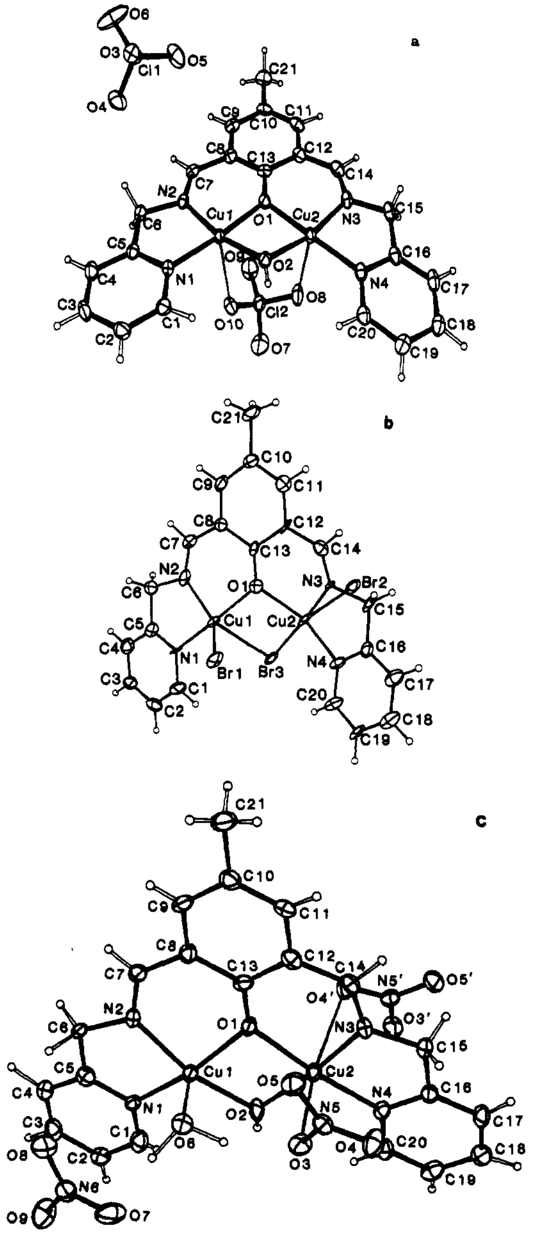

Figure 1. ORTEP perspective views of (a) $[Cu_2L(OH)](ClO_4)_2$, (b) $[Cu_2L(Br)]Br_2$, and (c) $[Cu_2L(OH)](NO_3)_2{\cdot}H_2O$, showing the atom-numbering schemes.

$[Cu_2L(OH)](NO_3)_2{\cdot}H_2O$. Each Cu^{II} ion is coordinated to two N atoms, and both the Cu^{II} ions are coordinated to the phenolic oxygen, O1, forming an O atom bridge, and are also bridged through another oxygen, O2, of the hydroxyl group. In addition, Cu1 is also coordinated to oxygen atom O6 of the water molecule [Cu1···O6 = 2.213 (4) Å] making it pentacoordinate whereas Cu2 is coordinated to two oxygen atoms occupying apical positions: atom O3 of the first nitrate group [Cu2···O3 = 2.712 (4) Å] (corresponding to N5) and O4 of a nitrate group symmetry related to the first ($^1/_2 + x, 1 - y, -^1/_2 + z$) [Cu2···O4 = 2.905 (4) Å]. Cu2 thus has an octahedral environment. Both the hydrogen atoms of the water molecule take part in hydrogen bonding, O6–H···O3 and O6–H···O7 ($^1/_2 + x, y, ^1/_2 + z$), of lengths 2.809 (5) and 2.722 (5) Å, respectively, forming a two-dimensional network parallel to the *ac* plane. These sheets are held together by several weak van der Waals contacts, and this is consistent with the fact that the crystals show sharp cleavage. Both the nitrate ions vibrate violently, as can be seen from the higher temperature factors of the O atoms.

Magnetic Analysis. The magnetic susceptibility data for complexes A, B, and C are plotted in Figure 2a–c, respectively. Each plot shows a maximum in the temperature-dependent magnetic susceptibility. This behavior is consistent with antiferromagnetic coupling between the two $S = ^1/_2$ copper(II) ions in the binuclear complexes. The data were analyzed with the equation

$$\chi = \frac{2Ng^2\mu_B{}^2}{kT}\,\frac{e^x}{1 + 3e^x} \tag{1}$$

where $x = 2J/kT$ and $2J$ represents the separation of the singlet

Table IV. Selected Bond Angles (deg)

atom 1	atom 2	atom 3	angle	atom 1	atom 2	atom 3	angle
			(a) $[Cu_2L(OH)](ClO_4)_2$ (Complex A)				
O1	Cu1	O2	78.73 (6)	O8	Cu2	N3	93.98 (6)
O1	Cu1	O10	94.36 (6)	O8	Cu2	N4	90.99 (6)
O1	Cu1	N1	175.19 (7)	N3	Cu2	N4	84.58 (7)
O1	Cu1	N2	91.62 (6)	O3	Cl1	O4	108.92 (9)
O2	Cu1	O10	86.09 (6)	O3	Cl1	O5	109.07 (9)
O2	Cu1	N1	104.63 (6)	O3	Cl1	O6	108.99 (9)
O2	Cu1	N2	167.82 (7)	O4	Cl1	O5	108.9 (1)
O10	Cu1	N1	89.33 (6)	O4	Cl1	O6	110.6 (1)
O10	Cu1	N2	102.18 (7)	O5	Cl1	O6	110.3 (1)
N1	Cu1	N2	84.58 (6)	O7	Cl2	O8	109.29 (9)
O1	Cu2	O2	78.96 (6)	O7	Cl2	O9	111.0 (1)
O1	Cu2	O8	86.43 (6)	O7	Cl2	O10	109.01 (9)
O1	Cu2	N3	92.04 (6)	O8	Cl2	O9	109.5 (1)
O1	Cu2	N4	175.60 (6)	O8	Cl2	O10	109.11 (8)
O2	Cu2	O8	94.46 (6)	O9	Cl2	O10	108.95 (9)
O2	Cu2	N3	167.23 (7)	Cu1	O1	Cu2	99.19 (6)
O2	Cu2	N4	104.83 (7)	Cu1	O2	Cu2	100.44 (7)
			(b) $[Cu_2L(Br)]Br_2$ (Complex B)				
Cu1	Br3	Cu2	75.50 (4)	Br2	Cu2	Br3	96.40 (5)
Br1	Cu1	Br3	96.60 (4)	Br2	Cu2	O1	107.9 (2)
Br1	Cu1	O1	94.6 (2)	Br2	Cu2	N3	87.6 (2)
Br1	Cu1	N1	101.5 (2)	Br2	Cu2	N4	104.0 (2)
Br1	Cu1	N2	134.0 (3)	Br3	Cu2	O1	87.0 (2)
Br3	Cu1	O1	80.4 (2)	Br3	Cu2	N3	175.5 (2)
Br3	Cu1	N1	92.4 (2)	Br3	Cu2	N4	99.6 (2)
Br3	Cu1	N2	129.2 (3)	O1	Cu2	N3	89.8 (3)
O1	Cu1	N1	163.0 (3)	O1	Cu2	N4	146.5 (3)
O1	Cu1	N2	90.2 (3)	N3	Cu2	N4	81.4 (3)
N1	Cu1	N2	82.5 (3)	Cu1	O1	Cu2	106.2 (3)
			(c) $[Cu_2L(OH)](NO_3)_2{\cdot}H_2O$ (Complex C)				
O1	Cu1	O2	77.6 (1)	O2	Cu2	N3	171.1 (2)
O1	Cu1	O6	88.2 (1)	O2	Cu2	N4	103.9 (2)
O1	Cu1	N1	165.6 (1)	O3	Cu2	O4′	165.1 (2)
O1	Cu1	N2	91.0 (2)	O3	Cu2	N3	85.1 (1)
O2	Cu1	O6	93.6 (1)	O3	Cu2	N4	92.8 (1)
O2	Cu1	N1	105.1 (2)	O4′	Cu2	N3	80.0 (2)
O2	Cu1	N2	164.9 (2)	O4′	Cu2	N4	85.4 (2)
O6	Cu1	N1	105.6 (1)	N3	Cu2	N4	84.6 (2)
O6	Cu1	N2	95.9 (2)	Cu1	O1	Cu2	99.9 (2)
N1	Cu1	N2	83.6 (2)	Cu1	O2	Cu2	102.2 (2)
O1	Cu2	O2	79.3 (1)	O3	N5	O4	120.1 (4)
O1	Cu2	O3	93.0 (1)	O3	N5	O5	118.2 (4)
O1	Cu2	O4′	88.2 (2)	O4	N5	O5	121.7 (4)
O1	Cu2	N3	92.5 (2)	O7	N6	O8	120.7 (5)
O1	Cu2	N4	173.3 (2)	O7	N6	O9	118.4 (5)
O2	Cu2	O3	91.7 (1)	O8	N6	O9	120.9 (4)
O2	Cu2	O4′	103.1 (1)				

Table V. Magnetic Parameters for Complexes of Formula $[Cu_2L(B)]^{2+}$ Obtained from Best Fit of the Magnetic Data to Eq 1 As Described in Text

	B	X	g	$2J$, cm^{-1}	TIP, emu/mol	% imp.
A	OH^-	ClO_4^-	2.05	−364	0.00006	0.7
B	Br^-	Br^-	2.03	−68	0.00012	1.5
C	OH^-	NO_3^-	2.10	−499	0.00008	0.6

Table VI. Magnetic and Structural Parameters for Complexes of Formula $[Cu_2L(B)]^{2+}$

B	X	$2J$, cm^{-1}	Cu–O–Cu, deg	Cu–B–Cu, deg	Cu–Cu, Å	Cu–O–Cu–B, deg
OH^-	ClO_4^-	−364	99.18	100.44	2.947	166.0
OH^-	NO_3^-	−499	99.90	102.2	2.991	170.0
Br^-	Br^-	−68	106.3	75.5	3.151	146.4
Cl^-	Cl^-	−84	105.9	87.0	3.169	175.5[27]

and triplet levels with a negative J denoting a ground singlet. In addition, the data were corrected for the presence of a small amount of paramagnetic impurity and the temperature-independent paramagnetism (TIP) of the copper(II) ions. The fitted parameters for each of the complexes are listed in Table V, and the curves drawn through the points in Figure 2a–c represent the best fit of eq 1 to the magnetic data of $[Cu_2L(OH)](ClO_4)_2$, $[Cu_2L(Br)]Br_2$, and $[Cu_2L(OH)](NO_3)_2{\cdot}H_2O$, respectively, from the parameters in Table V.

The deviation of the fitted curve from the magnetic data for $[Cu_2L(OH)](NO_3)_2{\cdot}H_2O$ (see Figure 2c) is the result of partial decomposition of the complex at high temperatures ($T > 325$ K). The crystalline decomposition is due to loss of the waters of crystallization in the complex. The data for complex C were therefore fit only at temperatures below the onset of decomposition ($T \leq 325$ K).

In Table VI, we have listed some structural parameters of the

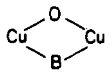

bridging skeleton along with the magnetic coupling parameter (from eq 1) for each of the copper(II) complexes of general formula $[Cu_2L(B)]^{2+}$. From the limited set of complexes listed in this table, we cannot propose a general correlation between magnetism and structure that will apply uniformly to all types of bridging ligands. Nevertheless, within a chemically defined class of bridging ligands, some previously discovered magnetostructural correlations do hold.

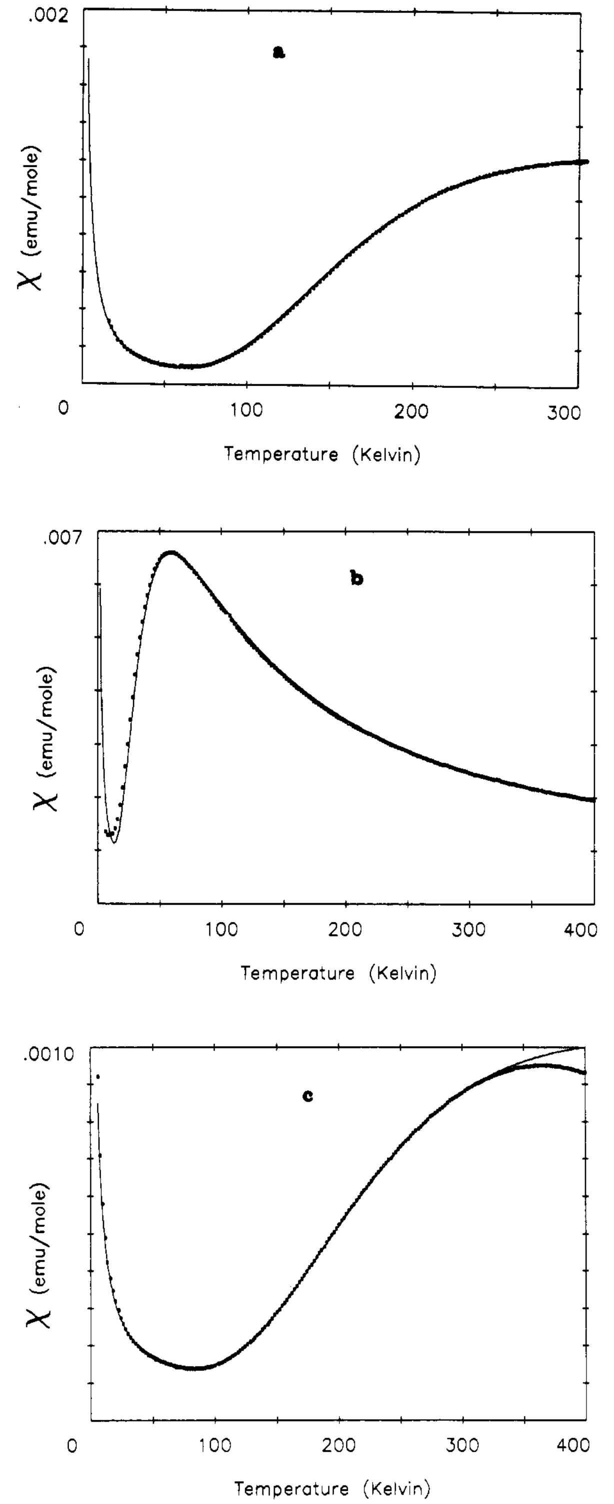

Figure 2. Magnetic susceptibility plotted as a function of temperature for (a) $[Cu_2L(OH)](ClO_4)_2$, (b) $[Cu_2L(Br)]Br_2$, and (c) $[Cu_2L(OH)](NO_3)_2 \cdot H_2O$. The curves through the data points are the best fit of the data to eq 1 as described in text using the parameters listed in Table V.

The most similar complexes listed in Table VI are the two hydroxide-bridged complexes (A and C). Both of these complexes exhibit relatively strong antiferromagnetic exchange between the two copper(II) centers. The average Cu–O–Cu bridging angles for these complexes are 99.8 and 101.1°, respectively. From the correlation discovered by Hatfield and Hodgson[29] for hydroxide-bridged complexes, a larger Cu–O–Cu bridging angle will give rise to a stronger antiferromagnetic coupling. This trend is followed for the two hydroxide-bridged complexes whether average angles or individual Cu–O–Cu bridging angles are compared.

A comparison of the chloride- and bromide-bridged complexes results in a stronger antiferromagnetic coupling observed in the chloride-bridged binuclear complex. However, the magnitude of the coupling in both halide-bridged species is significantly less than the coupling in the hydroxide-bridged species. At first glance, this is difficult to reconcile with the prediction of a strong antiferromagnetic component that would result from the large phenoxide bridging angle in both of the halide-bridged complexes.

The structural data of each of the complexes indicates there is a high degree of distortion about the copper(II). The five-coordinate geometry cannot be adequately described as either square pyramid or trigonal bipyramid, and in fact a more realistic interpretation of the coordination geometry lies between the two descriptions. If we assume that the trigonal-bipyramidal geometry dominates for these complexes and that the phenoxo bridge connects the two copper atoms through axial coordination, then the equatorial bridging atom will have the largest overlap with the $d_{x^2-y^2}$ orbital that contains the unpaired electron. This results in a primary exchange pathway via the exogenous bridge and negligible exchange via the phenoxide bridge. This explanation rationalizes the smaller coupling for the halide-bridged species, even though the phenoxo bridge is quite large and would otherwise contribute a large antiferromagnetic exchange if it were participating in the $d_{x^2-y^2}$ overlap exchange integral.

The larger antiferromagnetic coupling exhibited by the chloride relative to that of the bromide is expected. As shown by Gudel,[30] a theoretical analysis predicts a more efficient overlap integral for the chloride when the chloride and bromide are in equivalent bridging configurations.

In summary, it is apparent that the electron structure and the chemistry of the exogenous bridging ligand are the dominant factors governing the magnitude and sign of magnetic exchange. Purely structural effects become important only when the bridging ligands are chemically similar.

Acknowledgment. C.J.O. wishes to acknowledge a grant from the National Science Foundation (CHE 83-05707) for the purchase of a SQUID susceptometer and the E. G. Schleider Educational Foundation, the UNO Research Council, and the CNRS of France for support during the preparation of this report. C.J.O. also wishes to thank Prof. Olivier Kahn for many helpful discussions leading to the preparation of this paper.

Registry No. **1**, 7310-95-4; **2**, 102262-03-3; **3** (B = OH, X = ClO_4^-), 93358-28-2; **3** (B = X = Br^-), 102283-87-4; **3**·H_2O (B = OH, X = NO_3^-), 102262-02-2; 2-(aminomethyl)pyridine, 3731-51-9.

Supplementary Material Available: Tables of anisotropic thermal parameters for A–C, hydrogen atom positional parameters for B (calculated), all bond lengths and angles for A–C, magnetic susceptibility measurement data for A–C, and stereoscopic pairs of packing diagrams (24 pages). Ordering information is given on any current masthead page.

---

(29) Crawford, V. H.; Richardson, H. W.; Wasson, J. R.; Hodgson, D. J.; Hatfield, W. E. *Inorg. Chem.* **1976**, *15*, 2107. Hodgson, D. J. *Prog. Inorg. Chem.* **1975**, *19*, 173.

(30) Leuenberger, B.; Gudel, H. U. *Inorg. Chem.* **1986**, *25*, 181. Leuenberger, B.; Gudel, H. U.; Kjems, J. K.; Petitgrand, D. *Inorg. Chem.* **1985**, *24*, 1035.